33RD INTERNATIONAL COSMIC RAY CONFERENCE, RIO DE JANEIRO 2013
THE ASTROPARTICLE PHYSICS CONFERENCE

ICRC 2013

Galactic boron and carbon fluxes measured by the PAMELA experiment.

V. FORMATO[8,15], N. MORI[2], R. CARBONE[8], C. DE SANTIS[11,14], O. ADRIANI[1,2], G.C. BARBARINO[3,4], G.A. BAZILEVSKAYA[5], R. BELLOTTI[6,7], M. BOEZIO[8], E.A. BOGOMOLOV[9], M. BONGI[1,2], V. BONVICINI[8], S. BOTTAI[2], A. BRUNO[7], F. CAFAGNA[7], D. CAMPANA[4], P. CARLSON[10], M. CASOLINO[11,12], G. CASTELLINI[13], C. DE DONATO[10,11], M.P. DE PASCALE[11,14,*], N. DE SIMONE[11], V. DI FELICE[11], A.M. GALPER[16], A.V. KARELIN[16], S.V. KOLDASHOV[16], S. KOLDOBSKIY[16], Y. KRUTKOV[9], A.N. KVASHNIN[5], A. LEONOV[16], V. MALAKHOV[16], L. MARCELLI[14], M. MARTUCCI[14,17] A.G. MAYOROV[16], W. MENN[18], M. MERGÈ[11,14] V.V. MIKHAILOV[16], E. MOCCHIUTTI[8], A. MONACO[7], R. MUNINI[8,15], G. OSTERIA[4], F. PALMA[11,14], P. PAPINI[2], M. PEARCE[10], P. PICOZZA[11,14], C. PIZZOLOTTO[19,20,†], M. RICCI[17], S.B. RICCIARINI[2], R. SARKAR[8], M. SIMON[18], V. SCOTTI[3,4], R. SPARVOLI[11,14], P. SPILLANTINI[1,2], Y.I. STOZHKOV[5], A. VACCHI[8], E. VANNUCCINI[2], G. VASILYEV[9], S.A. VORONOV[16], Y.T. YURKIN[16], G. ZAMPA[8], N. ZAMPA[8], V.G. ZVEREV[16]

[1] *University of Florence, Department of Physics, I-50019 Sesto Fiorentino, Florence, Italy*
[2] *INFN, Sezione di Florence, I-50019 Sesto Fiorentino, Florence, Italy*
[3] *University of Naples "Federico II", Department of Physics, I-80126 Naples, Italy*
[4] *INFN, Sezione di Naples, I-80126 Naples, Italy*
[5] *Lebedev Physical Institute, RU-119991, Moscow, Russia*
[6] *University of Bari, Department of Physics, I-70126 Bari, Italy*
[7] *INFN, Sezione di Bari, I-70126 Bari, Italy*
[8] *INFN, Sezione di Trieste, I-34149 Trieste, Italy*
[9] *Ioffe Physical Technical Institute, RU-194021 St. Petersburg, Russia*
[10] *KTH, Department of Physics, and the Oskar Klein Centre for Cosmoparticle Physics, AlbaNova University Centre, SE-10691 Stockholm, Sweden*
[11] *INFN, Sezione di Rome "Tor Vergata", I-00133 Rome, Italy*
[12] *RIKEN, Advanced Science Institute, Wako-shi, Saitama, Japan*
[13] *IFAC, I-50019 Sesto Fiorentino, Florence, Italy*
[14] *University of Rome "Tor Vergata", Department of Physics, I-00133 Rome, Italy*
[15] *University of Trieste, Department of Physics, I-34147 Trieste, Italy*
[16] *NRNU MEPhI, RU-115409 Moscow, Russia*
[17] *INFN, Laboratori Nazionali di Frascati, Via Enrico Fermi 40, I-00044 Frascati, Italy*
[18] *Universitat Siegen, Department of Physics, D-57068 Siegen, Germany*
[19] *INFN, Sezione di Perugia, I-06123 Perugia, Italy*
[20] *Agenzia Spaziale Italiana (ASI) Science Data Center, I-00044 Frascati, Italy*
(*) Deceased
(†) Previously at INFN, Sezione di Trieste, I-34149 Trieste, Italy

valerio.formato@ts.infn.it

Abstract: The PAMELA experiment is a satellite-borne apparatus that performs measurements of the cosmic radiation with a particular focus on antiparticles and light nuclei. The heart of experiment is a magnetic spectrometer to measure the particle rigidity and sign of charge. A Time-of-Flight system, a Silicon-Tungsten calorimeter, and a neutron detector allow particle identification and lepton/hadron discrimination. The apparatus is surrounded by a set of anticoincidence scintillation counters to reject multi-particle events. In this work we will present the Boron and Carbon fluxes measured by PAMELA from July 2006 to March 2008. Such data, and in particular the B/C flux ratio, can help the modelling of the galactic cosmic rays propagation. This can be a crucial point in predicting the astrophysical background of antimatter (positrons and antiprotons) in cosmic rays in the search for a dark matter signal.

Keywords: icrc2013, cosmic-rays, galactic propagation.

1 Introduction

Measurements of the elemental composition of cosmic rays over a wide energy range are required in order to understand the origin, propagation and lifetime of the cosmic radiation. The primary cosmic rays (e.g. C and O), produced at the sources, propagate through the interstellar medium giving information about the composition at the source. Secondary elements (e.g. Li, Be, and B) are tracers of amount of matter traversed by the cosmic rays.

Abundances of secondary light nuclei (Li, Be and B) in cosmic rays are due to spallation of carbon and oxygen nuclei as they traverse the interstellar hydrogen. The amount of these elements determines the average thickness of interstellar matter which the radiation traverses and indicates an average lifetime of the cosmic rays in the galaxy of about 3 million years. Energy spectra of Li, Be and B are steeper than those of C and O, indicating that at higher energies nuclei do not undergo so much fragmentation, presumably because they leak out of the galaxy sooner than those lower energy [1], [2], [3], [4].

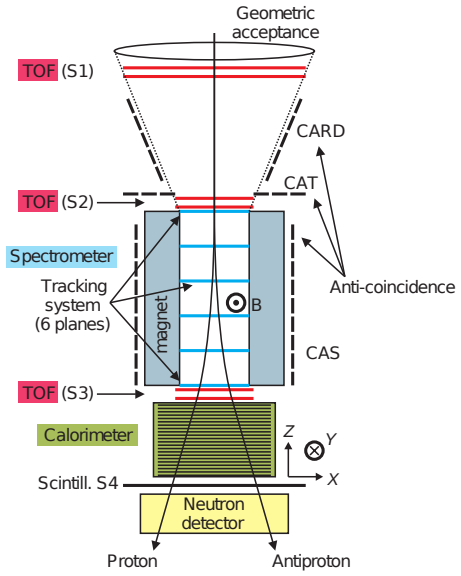

Fig. 1: A schematic overview of the PAMELA satellite experiment. The experiment stands ∼1.3 m high and, from top to bottom, consists of a time-of-flight (ToF) system (S1, S2, S3 scintillator planes), an anticoincidence shield system, a permanent magnet spectrometer (the magnetic field runs in the *y*-direction), a silicon-tungsten electromagnetic calorimeter, a shower tail scintillator (S4) and a neutron detector.

PAMELA (a Payload for Antimatter Matter Exploration and Lightnuclei Astrophysics)[5] is measuring the light nuclei component, up to oxygen, of the cosmic radiation since July 2006.

2 The PAMELA Apparatus

The PAMELA apparatus is housed inside a pressurized container attached to the Russian Resurs-DK1 satellite, which was launched on June 15th 2006. The orbit is elliptical and semi-polar, with an inclination of 70.0° and an altitude varying between 350 km and 610Km.
PAMELA comprises (from top to bottom as shown in Figure 1): a time-of-flight (ToF) system (S1, S2, S3), a magnetic spectrometer with silicon tracker planes, an anticoincidence system (CARD, CAT, CAS), an electromagnetic imaging calorimeter, a shower tail catcher scintillator (S4) and a neutron detector.

2.1 Time of Flight

The scintillator system provides trigger, charge and timeof-flight information. There are three scintillators layers, each composed of two orthogonal planes, divided into paddles (8 for S11, 6 for S12, 2 for S21 and S12 and 3 for S32 and S33).

2.2 Magnetic Spectrometer

The magnetic spectrometer is built around a permanent magnet composed of 5 blocks of segmented Nd-Fe-B alloy with a residual magnetization of 1.3 T. The size of the magnetic cavity is $13.1 \times 16.1 \times 44.5 cm^3$, with a mean magnetic field of 0.43 T. Six layers of 300 μm thick double-sided microstrip silicon detectors are used to measure particle deflection.

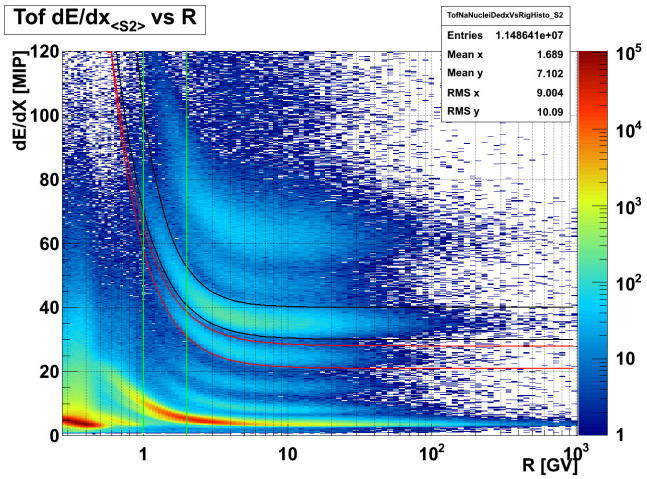

Fig. 2: Charge selection bands for boron (red) and carbon (black) on the mean energy release in S2 as a function of rigidity.

2.3 Anticoincidence System

Plastic anticoincidence scintillators allows to reject spurious triggers due to particles interacting with the body of the satellite. The CARD anticoincidence system comprises four 8 mm thick scintillators which bound the volume between S1 and S2. The CAT scintillator is placed on top of the magnet and has a central rectangular aperture corresponding to the magnet cavity. Four scintillators, arranged around the magnet, form the CAS lateral anticoincidence system.

2.4 Electromagnetic Imaging Calorimeter

The silicon tungsten sampling calorimeter provides topological and energetic information for particles which generate showers in the calorimeter, allowing lepton/hadron discrimination [7] and precise measurement of the energy of impinging electrons and positrons [8]. The calorimeter comprises 44 single-sided silicon planes (made of nine 380 μm thick, $8 \times 8 cm^2$ wide sensors) interleaved with 22 plates of tungsten absorbers, for a total depth of $16.3 X_0$ (0.6 nuclear interaction lengths).

2.5 Shower Tail Scintillator

This scintillator ($48 \times 48 \times 1 cm^3$) is located below the calorimeter and is used to improve hadron/lepton discrimination by measuring the energy not contained in the calorimeter and as a stand-alone trigger for the neutron detector.

2.6 Neutron Detector

The $60 \times 55 \times 15 cm^3$ neutron detector is composed of 36 ^3He tubes arranged in two layers and surrounded by polyethylene shielding and a U shaped cadmium layer to remove thermal neutrons not coming from the calorimeter. It is used to improve lepton/hadron identification by detecting the number of neutrons produced in the hadronic and electromagnetic cascades.

3 Data analysis

3.1 Basic event selections

These selections were developed in order to ensure a reliable event reconstruction and to select positively charged particles with a precise measurement of the absolute value of the particle rigidity and velocity.

Events with more than one track, likely to be products of hadronic interactions occurring in the top part of the apparatus, were rejected.

Particle rigidity has been obtained from the fit of the track in the spectrometer. For each particle, the tracking system provided up to 12 position measurements (6 in the bending view), which have been interpolated to form a trajectory described by integrating the equations of motion in the magnetic field.

Furthermore the selected track must be at least 1.5 mm away from the magnet walls and the reconstructed curvature has to be consistent with positively-charged particles. Selected tracks must have at least four hits in the bending view of the spectrometer and three hits in the non-bending view.

3.2 Charge Identification

The energy loss of a charged particle traversing matter is described by the Bethe-Bloch equation and it is proportional to the particle charge squared. A measurement of the average energy released the ToF planes for a given event at a given rigidity can therefore be used to distinguish between different particles. Boron and carbon candidates have been selected requiring energy loss compatible with Z=5 and Z=6 nuclei in each layer of a given combination (S12, S2, S3) of ToF planes. In Figure 2 the charge separation in the ToF system is shown.

3.3 Geomagnetic Selection

The local geomagnetic cutoff G has been evaluated using the Störmer approximation [9]. A value of $G = 14.9/L^2$ - valid for vertically incident particles - has been estimated using the IGRF magnetic field model along the orbit; from this the McIlwain L shell has been calculated [10]. Particles have been selected requiring $R > 1.3G$.

3.4 Top-of-payload corrections

The effect of hadronic interaction in the 2 mm aluminium container which houses PAMELA has been summarized in a correction factor, which accounts for non-elastic interactions and for the loss (gain) of particles from (within) the acceptance due to elastic scattering. This correction factor is almost constant above 3 GV and is shown in Figure 3

To correct the spectra distortion due to the resolution of the magnetic spectrometer and particle slowdown a Bayesian unfolding procedure, described in [13], was used to derive the number of events at the top of the payload (see also [14]).

4 Results

Boron and carbon fluxes were then derived as follows:

$$\Phi_{\mathrm{ToP}}(E) = \frac{N_{\mathrm{ToP}}(E)}{TG(E)\Delta E} \qquad (1)$$

where $N_{\mathrm{ToP}}(E)$ is the unfolded particle count for energy E, also corrected for all the selection efficiencies, ΔE is the energy bin width, and $G(E)$ is the effective geometrical factor (accounting also for particle loss due to inelastic scattering), and T the live time.

Results from this analysis will be shown at the conference.

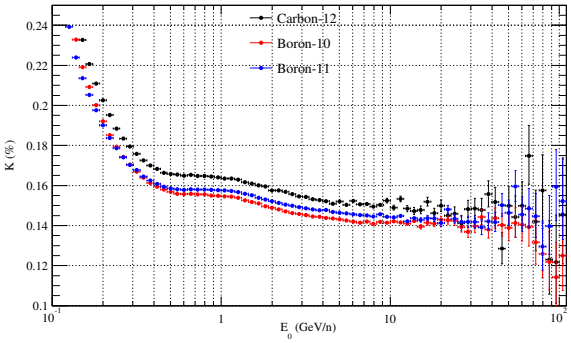

Fig. 3: Correction factor for particle lost due to inelastic scattering at the top of the payload.

References

[1] E. Juliusson, Astrophysical Journal, 1974, **191**: 331-348
[2] Orth, C. D. et. al., Astrophysical Journal, 1978, **226**(1): 1147-1161
[3] Swordy, S. P. et. al., Astrophysical Journal, 1990, **349**(1): 625633
[4] Engelmann, J. J. et. al., Astronomy and Astrophysics, 1990, **233**(1): 96-111
[5] Picozza, P. et. al., Astroparticle Physics, 2007, **27**(4): 296-315
[6] Adriani, O. et al., Science, 2011, **332**(6025): 69-72
[7] Boezio, M. et al., Astroparticle Physics, 2006, **26**(2): 111-118
[8] Boezio, M. et al., Nuclear Instruments and Methods in Physics Research Section A, 2002, **487**(3): 407-422
[9] Shea, M. A. et al., Physics of the Earth and Planetary Interiors, 1987, **48**(3-4): 200-205
[10] International geomagnetic reference field, Tech. rep., IAGA (2005)
[11] Wakely, S. P. et al., Advances in Space Research, 2008, **42**(3): 403-408
[12] Maestro, P. et al., Nuclear Physics B Proceedings Supplements, 2009, **196**: 239-242
[13] D'Agostini, G. 1995. *Nucl. Instrum. Meth.*, **A362**, 487.
[14] Adriani, O., *et al.* 2011. *Science*, **332**, 69 - Supplementary Online Material.